

# Strong stretching in dusk sector: stormtime activations and sawtooth events compared

N. Partamies, T. I. Pulkkinen, E. F. Donovan, H. J. Singer, E. I. Tanskanen, R. L. McPherron, M. G. Henderson, and G. D. Reeves

**Abstract:** Using superposed epoch analysis methods, we analyze two sets of events: one of stormtime activations having some characteristics of sawtooth events, and another set of events defined as sawtooth events. We compare and contrast these data sets and show that the sawtooth events are associated with slightly lower than average solar wind driving but the differences are small. While the both sets of events are associated with a positive excursion of the SYM-H index, the stormtime activations show a clearer signal in the ASY-H index highlighting the role of the partial ring current in such events. In the inner magnetotail, both sets of events show qualitatively similar injection and field dipolarization characteristics. We conclude that the repetition period of the sawtooth events is an internal property of the magnetosphere not related to the particular driving conditions that prevail during the sawtooth events.

*Key words:* stormtime substorms, sawtooth events.

## 1. Introduction

Sawtooth events are large-amplitude quasi-periodic oscillations of energetic particle fluxes and the magnetic field at geosynchronous orbit recurring with a period of about 2–4 hours [2, 4]. It is often reported that the particle injection is virtually simultaneous across several local time sectors (up to 12 hours). The events frequently occur embedded in magnetic storms when the solar wind driving is relatively strong and the interplanetary magnetic field (IMF) is continuously southward for a longer period of time. A distinct characteristic of these events is that the geosynchronous magnetic field can become highly stretched not only in the midnight sector but also in the evening sector reaching all the way to the dusk meridian and very close to the Earth [10]. An active debate is presently going on as to whether or not sawtooth events are recurring substorms [12] or a distinct class of activity.

Magnetospheric activity during storms is highly complex with strong fluctuations seen in a wide range of local time sectors. While some features (such as electrojet enhancements, geostationary orbit injections or tail field dipolarizations) sometimes resemble those found during non-storm substorms, at other times they do not: Not all stormtime activations identified from ground magnetometer data correspond to tail signatures typically associated with substorm; there are several types of stormtime activations of which only some resemble non-storm substorms [9].

In this paper, we analyze stormtime activations during the

year 2004. To address the question about whether sawtooth events form a special class of events, we also analyze a set of sawtooth events. We compare and contrast superposed epoch analysis results of both sets of events using measurements in the solar wind, in the geostationary orbit magnetosphere, and in the auroral and mid-latitude ionosphere.

## 2. Data set

A statistical analysis was performed for all storms with Dst less than  $-75$  nT during the year 2004. For each storm, ground magnetic recordings from the IMAGE network in the Scandinavian sector [18] and the CARISMA network in the Canadian sector [13] were visually examined to identify rapid electrojet enhancements exceeding about 200 nT. The activation onset was defined to be an electrojet enhancement on the ground. This analysis produced a list of 150 activations. For each of these events, the geosynchronous energetic electron fluxes and the geosynchronous magnetic field from the LANL and GOES satellites, the symmetric and asymmetric ring current indices (SYM-H, ASY-H) and the auroral electrojet (AL) index, as well as the solar wind parameters and the interplanetary magnetic field (IMF) from the ACE satellite [7, 15] were examined. In combining the results in the form of a superposed epoch analysis, an epoch time of three hours before and after the onset was used.

The geosynchronous magnetic field inclination is defined as the angle between the Earth's magnetic field vector and the equatorial plane in solar magnetic (SM) coordinates to best account for the differences in the dipole tilt angles for the different activations. In the SM coordinates, the Z axis is aligned with the dipole axis, X axis is in the plane defined by the dipole axis and the Sun-Earth line, and the Y axis completes the right-handed triad. The magnetometers onboard the GOES satellites provide a direct measurement of the magnetic field [14]; in addition, the electron anisotropy properties measured by the LANL magnetospheric plasma analyzers (MPA) were used to infer the field direction [17]. If the half-hour mean value of the inclination before and after the onset changed by more than

Received 14 May 2005.

**N. Partamies and E. F. Donovan.** Institute for Space Research, University of Calgary, Calgary, Alberta, Canada

**T. I. Pulkkinen, M. G. Henderson, and G. D. Reeves.** Los Alamos National Laboratory, Los Alamos, NM, USA

**H. J. Singer.** NOAA Space Environment Center, Boulder, CO, USA

**E. I. Tanskanen.** Finnish Meteorological Institute, Space Research, Helsinki, Finland

**R. L. McPherron.** Institute of Geophysics and Planetary Physics, UCLA, Los Angeles, CA, USA

four degrees, the event was categorized as having a magnetic field dipolarization associated with the electrojet enhancement. Similarly, if the half-hour average of the geosynchronous electron fluxes increased by a factor of two from before to after the onset, the event was categorized as having an injection. Note that this definition does not necessarily guarantee that the flux levels increase above the levels observed prior to the substorm growth phase.

Because of the rapidly recurring onsets, the time delays allowed for these to occur were limited to  $\pm 30$  minutes. Thus, a few events may have been misidentified as not having an injection or dipolarization due to the errors caused by the delays associated with particle drift times and/or substorm current wedge expansion times in the tail. For the same reason, the energetic particle injection study was limited to the rapidly drifting electrons. However, it is interesting to note that the injections and dipolarizations did not necessarily occur in the same local time sector. About a third of the stormtime activations did not show an injection or a dipolarisation at geosynchronous orbit simultaneously with the ground onset.

Our objective is to assess whether sawtooth events are in some identifiable way different from stormtime activations. Thus, we selected a subset of the stormtime activations that have characteristics most like the individual sawtooth onsets. Perhaps the most prominent characterizing property of the sawtooth events is strong field stretching at geosynchronous orbit extending to local times far duskward of the midnight sector. On this basis, we restricted our attention to the subset that consists of those stormtime activations (24 events) that showed extreme stretching in the dusk side magnetosphere. Our criterion was that the minimum inclination in the evening sector was less than  $30^\circ$ . We remind the reader that this subset is not comprised of sawtooth events, but rather events that resemble the individual activations during sawtooth events.

A similar superposed epoch analysis was performed for the same solar wind, geosynchronous, and ionospheric parameters for a set of 138 sawtooth events selected from the period 1999–2002.

### 3. Statistical results

#### 3.1. Solar wind parameters

A selection of the solar wind parameters for both data sets is shown in Fig. 1, where the superposed epoch analysis results of the stormtime activations (solid lines) are compared with the superposed epoch analysis results of the sawtooth events (dotted lines). The data measured by instruments onboard the ACE satellite located in the L1 point upstream of the Earth have been propagated to the magnetopause (to the distance of  $10 R_E$  upstream of the Earth) using the upstream distance of the satellite from the magnetopause and the average solar wind speed during that period.

The Z-component of the IMF (top panel) is more negative (by about 5 nT) during the stormtime activations. There is a clear minimum in  $B_z$  around the onset time for the stormtime activations. For the sawtooth events a less pronounced minimum occurs about half an hour prior to the onset time, which indicates that these sawtooth events are not, for the most part, triggered by IMF northward turnings.

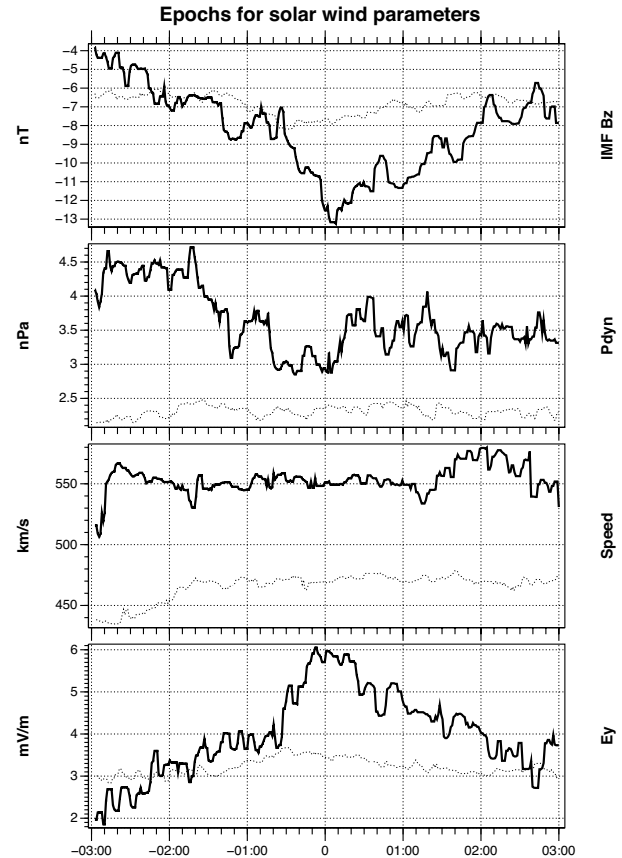


**Fig. 1.** Superposed epoch analysis of the IMF  $B_z$  (top), the solar wind dynamic pressure (second panel), velocity (third panel) and the Y component of the solar wind electric field (bottom). The stormtime activations are shown with solid lines and the sawtooth events are shown with dotted lines. All parameters are median filtered.

The solar wind dynamic pressure (second panel) changes are very small for both event sets varying between 2.0 and 4.5 nPa throughout the whole epoch. The solar wind velocities (third panel) are relatively steady, but the average speed for the stormtime activations is almost 100 km/s higher than for the sawtooth events.

The solar wind electric field (bottom panel) is stronger and more variable for the stormtime activations than for the sawtooth events. The typical behaviour of the electric field shows a maximum at the onset time for the stormtime activations, while the sawtooth related electric field is more steady showing a broad, slight, maximum during the hour before the event onset.

#### 3.2. Ionospheric activity

To study the ionospheric activity during the stormtime activations and the sawtooth events we analysed the asymmetric and symmetric ring current indices, ASY-H and SYM-H, as well as the local auroral electrojet (AL) index calculated from the CARISMA and IMAGE magnetometer networks. We call this the pseudo-AL index. These indices are plotted in Fig. 2.

ASY-H (top panel) shows only small fluctuations for the sawtooth events, but it is enhanced by about 20 nT around

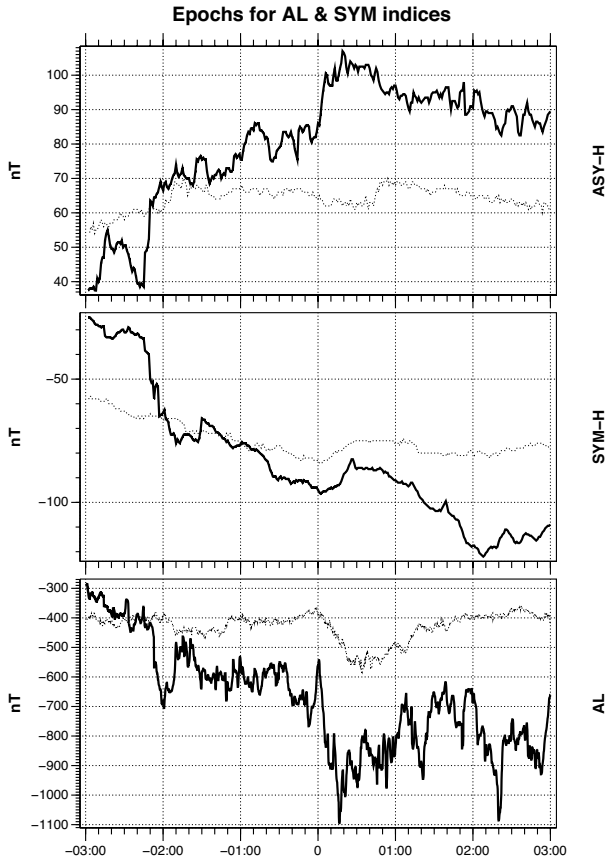


**Fig. 2.** Superposed epoch analysis of the asymmetric ring current index ASY-H (top), the symmetric ring current index SYM-H (middle), and the auroral electrojet index, the pseudo-AL (bottom). The stormtime activations are shown with solid lines and the sawtooth events are shown with dotted lines.

the onset of the stormtime activations. This indicates that the stormtime activations are more clearly associated with a strong partial ring current. SYM-H (middle panel) has a decreasing trend for the whole epoch of the stormtime activations. There is a similar increase in the index value at the onset time of both the sawtooth events (about 10 nT) and the stormtime activations (about 15 nT). Even though the partial ring current has been shown to be strongly enhanced during sawtooth events [10, 11], the superposed epoch result highlights the large-scale nature of both the sawtooth events and the stormtime activations with all local times showing injection and field dipolarization producing a positive effect at the mid-latitude ground magnetograms. The pseudo-AL index (bottom panel) shows a substorm-like decrease at onset for both data sets, but the negative deflection is several 100 nT deeper for the stormtime activations than it is for the sawtooth events. The onset-related decrease is also steeper for the stormtime activations than for the sawtooth events. For the stormtime activations the decrease is consistent with our selection criteria.

### 3.3. Geosynchronous observations

The magnetic field inclination changes and energetic particle injections were recorded by multiple spacecraft at geostationary orbit, in most cases giving a good local time coverage

around the Earth. For each event, each of the measuring satellites was binned into one of the five local time sectors: 12–18, 18–22, 22–02, 02–06 and 06–12 MLT. This allows us to examine the superposed epoch results in the different local time sectors separately. The results for the field inclination are shown in Fig. 3 and the electron data are shown in Fig. 4. As the satellites at different local times are also at different magnetic latitudes, the field inclination changes are not similar everywhere: a satellite at the equator would measure only a decrease in  $B_z$  but no change in field inclination, while a satellite off the equator would measure strong stretching and dipolarization of the field. Here we have made no attempt to correct for these differences; field inclinations are averaged as they were measured. For the electron data, the averages were computed using the logarithms of the fluxes to avoid domination of one or a few strong events.

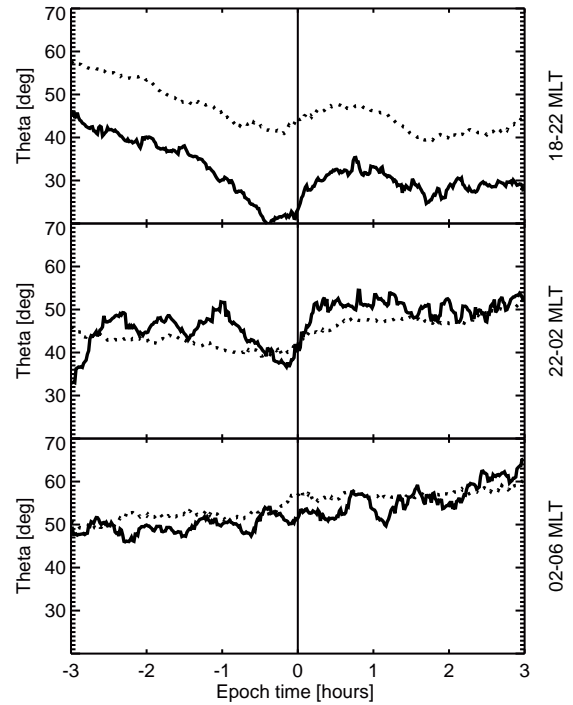


**Fig. 3.** Superposed epoch analysis of the field inclination angle at 18–22 MLT (top), 22–02 MLT (middle) and 02–06 MLT (bottom). The stormtime activations are shown with solid lines and the sawtooth events are shown with dotted lines.

By the selection process, the stormtime activations show a very stretched field in the evening sector prior to the onset. The average field dipolarizes rapidly at substorm onset returning to the average value preceding the growth phase. The dipolarization signature is clear also in the midnight sector. The morning-sector field inclination increases as well, although in that local time sector there is hardly any stretching of the field prior to the onset. The sawtooth events are characterized by strongest field stretching near midnight sector; the stretching–dipolarization cycle is clearly visible in the evening and midnight sectors. In

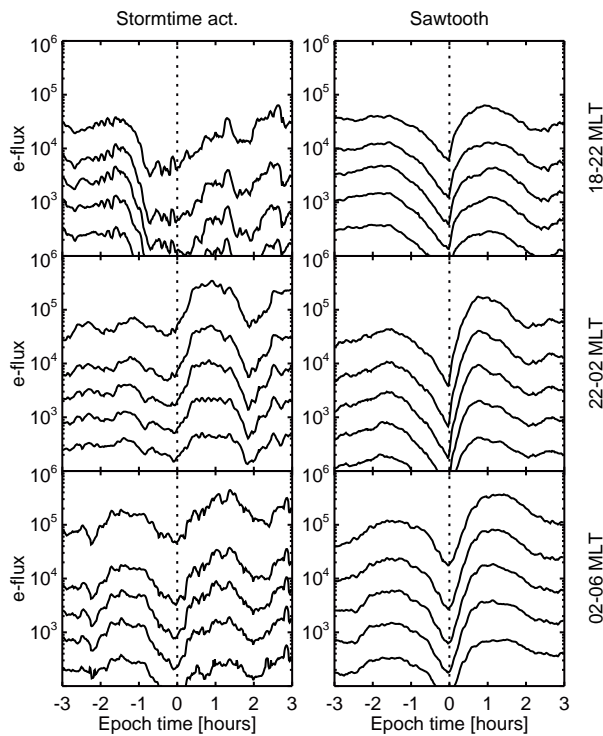


**Fig. 4.** Superposed epoch analysis of the energetic electron injections for the energies of 50–75, 75–105, 105–150, 150–225, 225–315 keV. The stormtime activations are shown in the left panels and the sawtooth events are shown in the right panels.

the morning sector, the field inclination shows a small jump beginning slightly before the onset time.

The injection characteristics for both stormtime activations and sawtooth events show very similar behaviour: There is a clear flux dropout observed at all local times in the hour preceding the onset, and almost simultaneous injections at all local times. Even the flux values are quite similar for both data sets indicating similarity in the overall field configuration (spacecraft mapping to similar radial distances in the equatorial plane). Interestingly, both data sets show a periodic signature with a prior injection about 2.5 hours prior to the selected onset time. This would indicate that the 2.5-hour periodicity reported in association with the sawtooth events is a more general feature of the magnetospheric activity (see also [3]).

#### 4. Discussion

We have analysed the typical behaviour of the solar wind parameters, IMF, geosynchronous magnetic field and injections as well as the ionospheric activity for a set of stormtime activations and sawtooth events. The sawtooth events were compared to the stormtime activations that most resemble observations during individual sawtooth injections: highly stretched dusk sector field followed by field dipolarization and injection over a wide local time sector (a subset of 24 events). The solar wind electric field and IMF  $B_z$  are on average somewhat stronger for the dusk sector stormtime activations than for the sawtooth

events. The solar wind speed is also clearly higher during the stormtime activations than during the sawtooth events. In the ionosphere, the stormtime activations are related to stronger activity as described by the pseudo-AL index. These events are also associated with more intense partial ring current than the sawtooth events. While by the selection criterion, the stormtime activation data set had stronger stretching in the evening sector, the geostationary orbit observations in general were very similar for both data sets.

The geostationary injection data show a periodicity with a prior activation about 2.5 hours earlier than the selected onset time. The signature is visible as well in the sawtooth event data as in the stormtime activation data. The latter indicates that the periodicity is perhaps related to an internal magnetospheric time scale. Interestingly, Borovsky et al. [3] find that averaged over all activity conditions, so-called periodic substorms recur at a rate of every 2.75 hours, very close to the values seen in both data sets studied here. The period is also similar to the recovery time of the substorm electrojets in the auroral ionosphere, while it is clearly longer than substorm recovery times in the midtail plasma sheet ( $\sim 20$  min) or at the geostationary orbit ( $\sim 90$  min) [8]. In the magnetotail, the key configuration change that is required before the onset is the formation of a thin current sheet in the inner part of the magnetotail [11]. During non-storm conditions, the growth phase time scale during which the current sheet intensifies sufficiently to allow the breakup instability to grow is about 30–60 min, i.e., much shorter than the recurrence period [6]. Thus, while the parameters controlling recurrence of magnetospheric activity remain unresolved, it seems that the recurrence period associated with sawtooth events is not a characteristic of this special class of events but a more general property of the Earth's magnetosphere.

The similarity of the driving conditions during stormtime activations and sawtooth events also points to a common origin of these events. The larger solar wind speed during the stormtime activations may either be a true effect or be due to the fact that the stormtime activations were selected during 2004, during the declining phase of the sunspot cycle. During the declining phase, there is a higher occurrence frequency of coronal high speed streams driving geomagnetic activity [5, 16]. However, it is the solar wind electric field rather than the solar wind speed itself that controls the level of geomagnetic activity [1]. As the driving electric field was quite similar for both cases, it would seem that the sawtooth events occur preferentially during slower speed and steadier  $B_z$ ; confirming this would require a larger dataset of both event types covering similar solar wind conditions.

Both sets of events tend to occur during decreasing SYM-H, i.e., storm main phases under strong driving. The sawtooth events and the stormtime activations show a similar positive deflection of the SYM-H, while the signature in ASY-H is strong during the stormtime activations and negligible during the sawtooth events. This indicates that the both sets of events have a wide local time range of the injection/dipolarization front. Even though case studies have shown the strong concentration of stretching in the evening sector [10], the sawtooth events seem to be better characterized by their large local time extent than by a concentration of activity in the evening sector. As the auroral electrojet activity is almost at a normal (non-

storm) substorm level [4], the resemblance of these activations to large substorms occurring close to the Earth is further emphasized.

In summary, the examination of stormtime magnetic activations shows that it is possible to select a subset of substorm-like activations in the ionosphere that have the characteristics in the driving solar wind, in geosynchronous field and particle measurements and auroral ionospheric currents that are very close to those observed during sawtooth events. Furthermore, the periodicity of the sawtooth events is repeated both in recurrent substorms and in stormtime activations, indicating that it is not a defining property of sawtooth events. We thus conclude that the sawtooth events are substorm-like activations that occur in sequence when the solar wind conditions are sufficiently constant to allow for the intrinsic magnetospheric time scales to control the activity repetition rate.

## Acknowledgments

The work of NP is supported by the Alberta Ingenuity Fund. TP thanks the IGPP for hosting her visit at Los Alamos. We thank the ACE MAG and SWEPAM instrument teams and the ACE Science Center for providing the ACE data. We also thank the LANL MPA team for the geosynchronous magnetic field data. ASY-H and SYM-H data were obtained from the World Data Center C2 in Kyoto.

## References

- Bargatze, L. F., Baker, D. N., McPherron, R. L., and Hones, E. W., Jr., Magnetospheric impulse response for many levels of geomagnetic activity, *J. Geophys. Res.*, *90*, 6387–6394, 1985.
- Belian, R. D., Cayton, T. E., and Reeves, G. D., Quasi-periodic global substorm-generated variations observed at geosynchronous orbit, in: *Space plasmas: Coupling between small and medium scale processes*, Geophys. Monogr., *86*, AGU, Washington DC 20009, 143, 1995.
- Borovsky, J. E., Nemzek, R. J., and Belian, R. D., The occurrence rate of magnetospheric-substorm onsets: random and periodic substorms, *J. Geophys. Res.*, *98*, 3807–3813, 1993.
- Henderson, M. G., Reeves, G. D., Skoug, R., Thomsen, M. F., Denton, M. H., Mende, S. B., Immel, T. J., Brandt, P. C., and Singer, H. J., Magnetospheric and auroral activity during the 18 April 2002 sawtooth event, *J. Geophys. Res.*, *111*, A01S90, doi:10.1029/2005JA011111, 2006.
- Mavromichalaki, H., Vassilaki, A., and Marmatsouri, E., A catalogue of high-speed solar wind streams: further evidence of their relationship to Ap-index, *Solar Phys.*, *115*, 345–365, 1988.
- McPherron, R. L., Growth phase of magnetospheric substorms, *J. Geophys. Res.*, *75*, 5592–5599, 1970.
- Ogilvie, K. W., Chorney, D. J., Fitzenreiter, R. J., Hunsaker, F., Keller, J., Lobell, J., Miller, G., Scudder, J. D., Sittler, E. C., Jr., Torbert, R. B., Bodet, D., Needell, G., Lazarus, A. J., Steinberg, J. T., Tappan, J. H., Mavretic, A., and Gergin, E., SWE, a comprehensive plasma instrument for the Wind spacecraft, *Space Sci. Rev.*, *71*, 55–77, 1995.
- Pulkkinen, T. I., Baker, D. N., Toivanen, P. K., Pellinen, R. J., Friedel, R. H. W., and Korth, A., Magnetospheric field and current distributions during the substorm recovery phase, *J. Geophys. Res.*, *99*, 10955–10966, 1994.
- Pulkkinen, T. I., Koskinen, H. E. J., Kauristie, K., Palmroth, M., Reeves, G. D., Donovan, E., Singer, H. J., Slavin, J. A., Russell, C. T., and Yumoto, K., Storm-substorm coupling: Signatures of stormtime substorms, Proceedings of the Conference in Memory of Yuri Galperin, CAUSES Handbook-1, edited by L. M. Zelenyi, M. A. Geller and J. H. Allen, Boulder, 309–316, 2004.
- Pulkkinen, T. I., Ganushkina, N. Yu., Tanskanen, E. I., Kubyskhina, M., Reeves, G. D., Russell, C. T., Singer, H. J., and Slavin, J. A., Magnetospheric current systems during stormtime sawtooth events, *J. Geophys. Res.*, *in press*, 2006.
- Pulkkinen, T. I., Goodrich, C. C., and Lyon, J. G., Thin current sheets as part of the substorm process, *this issue*, 2006.
- Reeves, G. D., Henderson, M. G., Skoug, R. M., Thomsen, M. F., Borovsky, J. E., Funsten, H. O., Brandt, P. C., Mitchell, D. J., Jahn, J.-M., Pollock, C. J., McComas, D. J., and Mende, S. B., IMAGE, POLAR, and geosynchronous observations of substorms and ring current ion injection, in *Disturbances in Geospace: The Storm-Substorm Relationship*, Geophys., Monogr. Ser., vol. 142, edited by A. S. Sharma et al., 89–100, AGU, 2004.
- Rostoker, G., Samson, J. C., Creutzberg, F., Hughes, T. J., McDiarmid, D. R., McNamara, A. G., Vallance Jones, A., Wallis, D. D., and Cogger, L. L., CANOPUS - a ground-based instrument array for remote sensing the high latitude ionosphere during the ISTP/GGS program, *Space Sci. Rev.*, *71*, 743–760, 1995.
- Singer, H. J., Matheson, L., Grubb, R., Newman, A., and Bouwer, S. D., Monitoring space weather with the GEOS magnetometers, SPIE conference proceedings, vol. 2812, 299–308, *GEOS-8 and Beyond*, edited by R. Edward, Washwell, 1996.
- Smith, C. W., Heures, J. L., Ness, N. F., Acuna, M. H., Burlaga, L. F., and Scheifele, J., The ACE magnetic fields experiment, *Space Sci. Revs.*, *86*, 613–632, 1998.
- Tanskanen, E. I., Slavin, J. A., Tanskanen, A. J., Viljanen, A., Pulkkinen, T. I., Koskinen, H. E. J., Pulkkinen, A., and Eastwood, J., Magnetospheric substorms are strongly modulated by interplanetary high-speed streams, *Geophys. Res. Lett.*, *32*, L16104, doi:10.1029/2005GL023318, 2005.
- Thomsen, M. F., McComas, D. J., Reeves, G. D., and Weiss, L. A., An observational test of the Tsyganenko (T89a) model of the magnetospheric field, *J. Geophys. Res.*, *101*, 24827–24836, 1996.
- Viljanen, A. and Häkkinen, L., IMAGE magnetometer network. In: *Satellite-Ground Based Coordination Sourcebook* (editors: M. Lockwood, M. N. Wild and H. J. Opgenoorth). ESA publications SP-1198, 111–117, 1997.

